AGU PUBLICATIONS

JGR

Journal of Geophysical Research: Oceans

RESEARCH ARTICLE

10.1002/2016JC011703

Key Points:
- DVM in Young Sound persisted throughout the entire winter including the period of polar night
- Polynya-enhanced circulation disrupted DVM favoring zooplankton to occupy the surface layer
- Weaker intensity of DVM beneath ice during polar night was observed when the moon was in full phase

Correspondence to:
V. Petrusevich,
vlad.petrusevich@umanitoba.ca

Citation:
Petrusevich, V., I. A. Dmitrenko, S. A. Kirillov, S. Rysgaard, S. Falk-Petersen, D. G. Barber, W. Boone, and J. K. Ehn (2016), Wintertime water dynamics and moonlight disruption of the acoustic backscatter diurnal signal in an ice-covered Northeast Greenland fjord, *J. Geophys. Res. Oceans*, *121*, 4804–4818, doi:10.1002/2016JC011703.

Received 22 FEB 2016
Accepted 3 JUN 2016
Accepted article online 9 JUN 2016
Published online 16 JUL 2016

Wintertime water dynamics and moonlight disruption of the acoustic backscatter diurnal signal in an ice-covered Northeast Greenland fjord

Vladislav Petrusevich[1], Igor A. Dmitrenko[1], Sergey A. Kirillov[1], Søren Rysgaard[1,2,3], Stig Falk-Petersen[4,5], David G. Barber[1], Wieter Boone[1], and Jens K. Ehn[1]

[1]Centre for Earth Observation Science, University of Manitoba, Winnipeg, Manitoba, Canada, [2]Greenland Climate Research Centre, Greenland Institute of Natural Resources, Nuuk, Greenland, [3]Arctic Research Centre, Aarhus University, Aarhus, Denmark, [4]Faculty of Biosciences, Fisheries and Economics, UiT The Arctic University of Norway, Tromsø, Norway, [5]Akvaplan-niva, Fram Centre for Climate and the Environment, Tromsø, Norway

Abstract Six and a half month records from three ice-tethered Acoustic Doppler Current Profilers deployed in October 2013 in Young Sound fjord in Northeast Greenland are used to analyze the acoustic backscatter signal. The acoustic data suggest a systematic diel vertical migration (DVM) of scatters below the land-fast ice during polar night. The scatters were likely composed of zooplankton. The acoustic signal pattern typical to DVM persisted in Young Sound throughout the entire winter including the period of civil polar night. However, polynya-enhanced estuarine-like cell circulation that occurred during winter disrupted the DVM signal favoring zooplankton to occupy the near-surface water layer. This suggests that zooplankton avoided spending additional energy crossing the interface with a relatively strong velocity gradient comprised by fjord inflow in the intermediate layer and outflow in the subsurface layer. Instead, the zooplankton tended to remain in the upper 40 m layer where relatively warmer water temperatures associated with upward heat flux during enhanced estuarine-like circulation could be energetically favorable. Furthermore, our data show moonlight disruption of DVM in the subsurface layer and weaker intensity of vertical migration beneath snow covered land-fast ice during polar night. Finally, by using existing models for lunar illuminance and light transmission through sea ice and snow cover, we estimated under ice illuminance and compared it with known light sensitivity of Arctic zooplankton species.

1. Introduction

Diel vertical migration (DVM) of zooplankton is a process of synchronized movement of the organisms from the mesopelagic zone up to the epipelagic zone at night and returning back during the day [*Brierley*, 2014]. DVM is considered to be the largest synchronized diel movement of biomass on the planet. It also acts as a biological pump in transferring organic carbon from the surface of the ocean to depth [*Doney and Steinberg*, 2013]. There are few probable reasons for DVM [*Hays*, 2003; *Ringelberg*, 2010]. First of all, vertical migration provides metabolic or demographic advantage in predator avoidance [*Zaret and Suffern*, 1976; *Kerfoot*, 1985; *Torgersen*, 2003]. Staying away from surface waters during day reduces the light-dependent mortality risk. Additional possible driving mechanism is the optimization of the exploitation of food resources [*Lampert*, 1989].

Most earlier studies of DVM in the Arctic have focused on the period of midnight sun or the transition period from midnight sun to day/night cycle [*Kosobokova*, 1978; *Fortier*, 2001; *Blachowiak-Samolyk et al.*, 2006; *Cottier et al.*, 2006; *Falk-Petersen et al.*, 2008; *Rabindranath et al.*, 2010]. Recent studies based on acoustic backscatter (ABS) data showed presence of synchronized DVM behavior of zooplankton that continued throughout the Arctic winter, in both open as in ice-covered waters [*Berge et al.*, 2009, 2012, 2015a, 2015b; *Benoit et al.*, 2010; *Wallace et al.*, 2010; *Båtnes et al.*, 2015; *Cohen et al.*, 2015]. *Berge et al.* [2014] proposed that, even during polar night, DVM is regulated by diel variations in solar and lunar illumination, which are at intensities far below the threshold of human perception. Alternatively DVM could be controlled by precise internal clocks. However, this would require a clock imprint or clock learning in earlier life stages when plankton live closer to the surface [*van Haren and Compton*, 2013]

While significant progress has been made in understanding DVM and its driving mechanisms, the oceanographic forcing interaction with of DVM in high latitude waters remains poorly understood. Vertical density stratification and water dynamics along with sea-ice cover are among the most important factors that seem to be capable to modify the regular patterns of DVM [*Berge et al*., 2014]. Arctic fjords with relatively isolated water columns exposed to the interaction with the shelf only through the fjord entrances, allow clear attribution of the oceanographic forcing and therefore represent an excellent research laboratory for investigating the impact of the oceanographic forcing on DVM.

The estuarine-like two-layer circulation is a typical pattern of the fjord water dynamics [*MacCready and Geyer*, 2009; *Stigebrandt*, 2012]. It is comprised by an outward flowing surface layer and an inward compensating flow at intermediate depths [*Farmer and Freeland*, 1983; *Skarðhamar and Svendsen*, 2010; *Sutherland et al*., 2014]. For the high Arctic fjords without subglacial discharge, and where freshwater runoff is relatively small and limited to a few summer months, inflow of intermediate-depth waters into the fjord is often in response to wind forcing where there is an enhanced estuarine-type flow pattern with down-fjord winds [*Cottier et al*., 2010]. For the silled fjords, the compensating inflow from the shelf is impeded by the entrance sill representing a topographic barrier. Therefore sills play an important role with respect to water structure, circulation, and biology, slowing replenishment of a fjord's intermediate and deep layers with more oxygenated water [*Dmitrenko et al*., 2015].

The acoustic Doppler current profiler (ADCP) is a commonly used instrument for velocity profiling in the water column. Besides velocity profiles, it measures the intensity of acoustic pings backscattered by suspended particles. An ADCP can be used with some limitations (due to the beam geometry) for measuring zooplankton abundance [*Flagg and Smith*, 1989; *Stanton et al*., 1994; *Brierley et al*., 1998, 2006; *Deines*, 1999; *Fielding et al*., 2004; *Lemon et al*., 2008].

Here we examine the DVM behavior during polar night and its interaction with water dynamics using time series of acoustic and velocity data obtained in the Young Sound (YS) fjord in Northeast Greenland at ~74°N. YS represents a relatively deep (340 m) and long (~90 km) high latitude fjord with a water depth of 40 m at the sill at its mouth. Land-fast ice covers the fjord from late October to beginning of July [*Bendtsen et al*., 2007]. During winter, the land-fast ice extends off the YS mouth by 10–30 km and completely eliminates wind stress to the water column. Based on oceanographic observations using three land-fast ice-tethered oceanographic moorings deployed from October 2013 to May 2014, we show that the DVM signal was disrupted below the land-fast ice when a polynya opened over the YS outlet to the Greenland Sea and caused enhanced surface layer (0–40 m) transport toward the mouth of the fjord and inflow to the fjord in a layer below (~40–140 m) [*Dmitrenko et al*., 2015]. We also show that DVM below the 60–90 cm thick land-fast sea ice and up to 50 cm of snow cover was affected by the moon cycle during polar night showing a disrupted signal in the subsurface layer and a generally weaker intensity of vertical migrations at the full moon phase.

We note that our analysis is entirely based on the ADCP data. In YS, zooplankton sampling during winter has never been accomplished due to logistical difficulties, and the zooplankton species comprising DVM are only hypothesized based on the 300 KHz ADCP sensitivity to scatters having a diameter greater than about 1.5 mm. Thus, the interpretation of the observed DVM patterns follows those reported using representative observations in other regions.

2. Data and Methods

2.1. Mooring Setup

Between October 2013 and May 2014, four land-fast ice-tethered moorings were deployed from the stationary land-fast ice in YS (Figure 1). All moorings included 300 kHz downward-looking Workhorse Sentinel ADCPs by Teledyne RD Instruments, mounted in 2 m long land-fast ice-tethered PVC pipes, with their acoustic transducer heads placed at 2 m below the sea surface. The velocity and acoustic backscatter (ABS) intensity data from the ADCPs were taken at 2 m depth intervals, with a 10-min ensemble time interval and 20 pings per ensemble. The first/last bins were located at 6/84 m except for mooring *m02* where the last valid bin was at 78 m. Therefore, the ADCPs did not sample the 5 m thick subsurface layer below the land-fast ice. The tilt of all ADCPs remained constant during the entire period of deployment

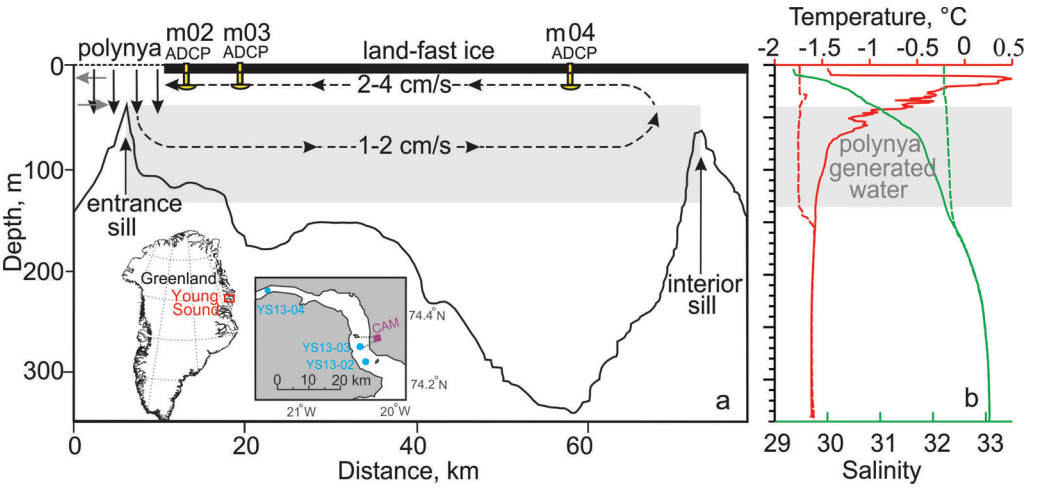

Figure 1. (a) Schematic depiction of polynya impact on the YS circulation adapted from *Dmitrenko et al*. [2015]. The first map insert shows Young Sound (YS) on the Greenland map and the second map shows positions of landfast ice-tethered oceanographic moorings (red circles) deployed in YS from October 2013 to May 2014 and position of time lapsed camera (purple square) facing mooring *m3*. (b) Vertical distribution of temperature (red, °C) and salinity (green) in 26 October2013 (solid lines, temperature and salinity only) and 5 May 2014 (dashed lines) at mooring *m04*.

and did not exceed 1° in any of them. Mooring *m01* was lost when the land-fast ice broke up over the YS mouth in December 2013 [*Dmitrenko et al*., 2015].

In many cases, the particles in the water column responsible for a significant portion of the ABS are planktonic. Based on theoretical analysis by *Jasek and Marko* [2007], our 300 kHz ADCPs are sensitive to particles having diameters greater than about 1.5 mm, which in general is consistent with small mesozooplankton species. However, sound scattering by zooplankton is more complex compared to that by sediment particles [*Stanton et al*., 1994]. Nevertheless, the acoustic backscatter has been found to be correlated to zooplankton biomass [*Flagg and Smith*, 1989; *Brierley et al*., 1998; *Fielding et al*., 2004; *Berge et al*., 2009; *Hamilton et al*., 2013; *Bozzano et al*., 2014]. It was noted, however, that ADCPs, unlike echo-sounders, are limited in deriving accurate quantitative estimates of biomass due to calibration difficulties because their acoustic beams are narrow and are inclined to the vertical [*Sato et al*., 2013; *Vestheim et al*., 2014; *Brierley et al*., 1998]. With application of beam geometry correction, ADCPs are commonly used for qualitative studies of biomass, as they can provide information on zooplankton behavior [e.g., *Pinot and Jansá*, 2001; *Chenghao et al*., 2013]. To correct for beam geometry we derived volume backscatter strength (VBS) S_v in dB from echo intensity following the procedure described by *Deines* [1999]. The ADCP-derived vertical velocity has also been used to study rates of zooplankton diel vertical migration [e.g., *Plueddemann and Pinkel*, 1989; *Cottier et al*., 2006; *Ochoa et al*., 2013]. In our data set the ADCPs velocity precision and resolution were ±0.5% and ±1 mm/s, respectively. The estimated ADCP velocity error was 15.5 mm/s. The accuracy of the ADCP vertical velocity measurements has not been verified. The manufacturer reports that the vertical velocity is more accurate, by at least a factor of two, than the horizontal velocity, however, vertical velocities in the 3 mm/s range may well be within the noise level [*Miller et al*., 2003]. Compass accuracy is reported as ±2.7° and was corrected by adding magnetic deviation (−18.5°).

The mooring-based observations were complemented by conductivity-temperature-depth (CTD) profiling during the deployment and recovery of moorings (Figure 1b) with an SBE-19plus (Sea-Bird Electronics). According to the manufacturers' estimates, the SBE-19plus individual temperature and conductivity measurements are accurate to ±0.005°C and ±0.0005 S/m.

2.2. Snow and Ice Thickness and Illumination During Polar Night

In addition, an ice-mass balance buoy (IMB) [*Babb et al*., 2016; *Kirillov et al*., 2015] deployed at the *m04* position in October 2013 provided data on ice thickness and snow depth every 30 min until the system was recovered in May 2014 (for more details see *Kirillov et al*. [2015]). The main components of the IMB were the thermistor string installed in a PVC housing and two precisely mounted acoustic rangefinders (above ice cover and beneath ice cover underwater, both with accuracy of 5 mm). The system works by measuring the

Figure 2. Pictures taken during the 2013–2014 civil twilight and civil polar night by camera facing mooring *m03*. All pictures were taken at local solar noon. Credits: the monitoring program MarineBasis Zackenberg (www.Zackenberg.dk).

distance from each rangefinder to either the snow/air or underwater ice/water interface, which allows the estimations of snow accumulation onto the ice surface and the growth of the ice cover (Figure 2a).

The lengths of daylight and twilight were calculated using trigonometry equations (http://www.gandraxa.com/length_of_day.xml). Modeled total sky illumination for day and night was calculated using skylight.m function from the astronomy package for Matlab [*Ofek*, 2014]. Modeled under ice illumination was calculated using exponential decay radiative transfer model [*Grenfell and Maykut*, 1977; *Perovich*, 1996]. Transmittance through the sea ice and snow cover was calculated using the following equation: $T(z)=i_0e^{-k_tz}$, where i_0 is the is the fraction of the wavelength-integrated incident irradiance transmitted through the top 0.1 m of the surface layer, and κ_t is the total extinction coefficient in the snow or sea ice cover. The values adopted for the sea ice and snow covers were $i_0 = 0.63$, $\kappa_t=1.5$, and $i_0 = 0.9$, $\kappa_t=0.1$, respectively.

For monitoring ice, snow and illumination conditions and visual verification, a time lapse camera was installed in the mouth of fjord overlooking mooring *m03*. The camera takes daily pictures at local solar noon (Figure 2). The total cloud cover (%) for the YS region at 75°N and 20°E is obtained from the National Centers for Environmental Prediction (NCEP).

For the analysis of acoustic backscatter data, we used wavelet transformation to derive the time-dependent behavior of the acoustic backscatter at the diurnal frequency band that dominates the backscatter spectrum. The wavelet transform method is used to analyze time series that contain nonstationary power at different frequencies. The results of the wavelet transform allow the spectral composition of nonstationary signals to be measured and examined [*Kumar and Foufoula-Georgiou*, 1997]. In this study we use the Morlet wavelet [*Morlet et al*., 1982a, 1982b].

2.3. Oceanographic Condition

The tide-dominated periodical water dynamics is relatively weak in YS. Tidal analysis conducted using an algorithm by *Foreman* [1978] for the velocity record shows the predominant M_2 constituent with velocity amplitudes of 0.89/2.86/5.78 cm/s, and S_2 constituent with velocity amplitudes of 0.38/1.14/2.49 cm/s for moorings *m04/m03/m02* (Figure 1). Thus, it was found that tidal dynamics were weakened toward the YS interior, and were nearly free of horizontal tidal movement at *m04*.

During winter 2013–2014, the nonperiodical water dynamics in YS was dominated by the estuarine-like circulation with inflow of water between 40 m and 140 m (beneath the level of the entrance sill) toward the interior of the fjord with a corresponding outflow in the 0–40 m surface layer (Figures 1a, 3b, 3e, and 3d). A storm event on 18–25 December 2013, with northerly winds reaching up to 25 m/s, forced the collapse of the land-fast ice over the YS outlet to the Greenland Sea on 20 December [*Dmitrenko et al*., 2015]. This

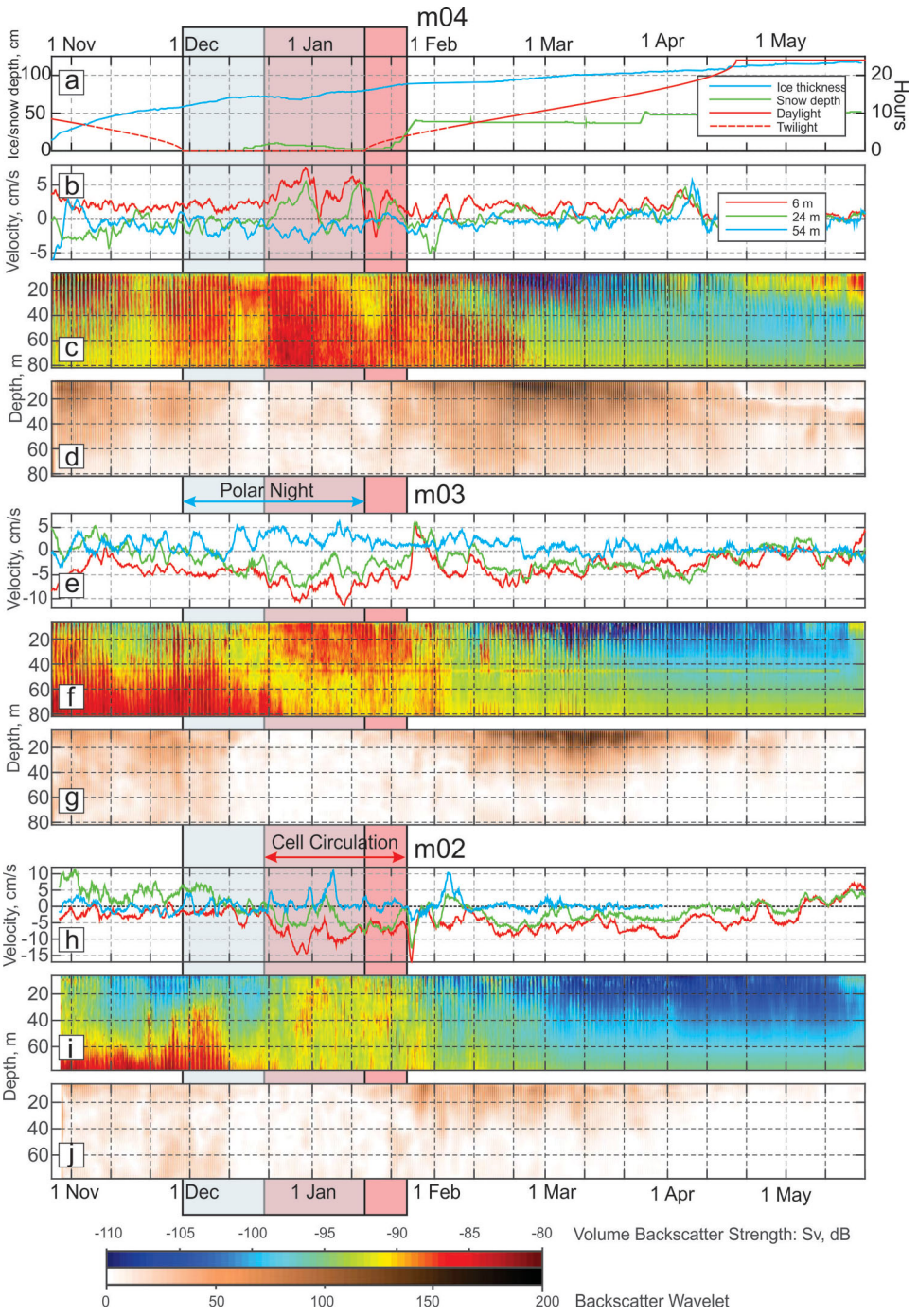

Figure 3. (a) The time series of (red) snow and (blue) ice thickness (cm) at *m04* and (green) duration of (solid) sunlight + (dashed) civil twilight (h); (b, e, h) The time series of along-fjord velocity at (red) 6 m, (green) 24 m, and (blue) 54 m for moorings *m04, m03*, and *m02*, respectively; (c, f, i) The time series of 2-m binned vertical profiles of acoustic backscatter for moorings *m04, m03*, and *m02*, respectively; (d, g, j) The absolute value of wavelet power spectrum for the time series of acoustic backscatter computed for diurnal frequency band (24 h) as a function of depth for moorings *m04, m03*, and *m02*, respectively. Blue and pink shading highlights polar night and enhanced cell circulation, respectively. Vertical black dashed line depicts winter solstice.

December storm created a coastal polynya that was maintained until early March 2014 by several consecutive strong northerly wind events that exceeded 15 m/s. Brine rejection associated with new ice formation in the polynya was most efficient during the first polynya event from 20 December 2013 to 23 January 2014 when the outer fjord salinity at ~80 m increased from 31.9 to 32.1 [*Dmitrenko et al.*, 2015]. The gravity current of dense and brine-enriched polynya-modified water enhanced the circulation cell

with inflow and outflow velocities exceeding 7 and 12 cm/s, respectively (Figures 3b, 3e, and 3d). This supplied the YS interior with cool, saline (Figure 1b) and oxygen enriched (not shown) polynya-modified water [*Dmitrenko et al*., 2015]. In the following, we show that the enhanced estuarine-like circulation cell affected the irregularities of the acoustic backscatter diurnal variability by disrupting its seasonal tendency associated with seasonality of light conditions at high latitudes.

3. Results

3.1. Acoustic Backscatter Intensity Time Series

The civil polar night period (nautical twilight) for YS at 74.4°N lasted from 28 November to 10 January, while civil twilight lasted from 3 November to 3 February (Figures 2 and 3a). Civil polar night occurs in the latitudinal range between 72°N and 78°N when the sun is between 6° and 12° below the horizon. Even though YS is located south of 78° zone of nautical polar night latitudes [*Berge et al*., 2015a], the illumination in the fjord interior (mooring *m04*) remained close to that of the nautical polar night due to the significant shadowing effect of the ~1000 m high mountains bordering the fjord. The modeled levels of maximum solar illumination at noon during the civil polar night period were around 0.2 lux, which are comparable with the maximal modeled lunar illumination of 9×10^{-2} lux. The modeled levels were estimated without taking into consideration shading by the mountains or attenuation due to the cloud cover.

The time series of the VBS from the moorings *m02* and *m03*, located near the mouth of fjord, show maxima in backscattering at depths beneath 40 m until 20 December (Figure 3). After that a period of enhanced circulation commenced and lasted until 23 January. During this period, both moorings showed the maximum backscatter in the subsurface layer (6–40 m) decreasing with depth (Figures 3f and 3i). For mooring *m04*, located in the fjord interior, the VBS pattern was almost reverse. For the period preceding the winter solstice, maximum backscatter at *m04* was located in the subsurface layer while after, and especially during the cell circulation the high backscatter was detected throughout the water column with some decrease in the subsurface layer by the end of cell circulation period. A general tendency of acoustic backscatter to decrease from the YS interior (*m04*) to the YS mouth (*m02*) was also noted. For *m03* there was a backscatter noise signal at 45m caused by CTD sensor located at the mooring line.

The wavelet spectrum shows general patterns of the diurnal periodicity for the VBS during winter 2013-2014. Similar to *VBS*, its diurnal variability was most intense at *m04* and decreased toward the YS mouth (Figures 3d, 3g, and 3j). The intensity of diurnal signal was gradually weakened during the civil twilight preceding polar night. During polar night, however, it still remained recognizable with 1/3 (*m02*) to 1/7 (*m04*) of the amplitude of the preceding civil twilight period (Figures 3d, 3g, and 3j). We note that this diurnal signal was observed below the 0.6–0.8 m thick land-fast ice with a ~10–15 cm snow cover (Figure 3a). During the civil twilight period following the polar night, the intensity of the diurnal signal increased. Overall, for all three moorings, the diurnal signal displayed a weakening trend from the start of polar night until winter solstice (~15 days) and then increased toward the end of polar night. For the 20–40 m depth layer, the return to the initial strength of diurnal signal at the beginning of polar night (i.e., ~75–100) took about 32 days following winter solstice (Figures 3d, 3g, and 3j). This asymmetry around the winter solstice can hardly be attributed to the higher rate of light attenuation due to the sea-ice growth in polar night from ~60 to 80 cm (Figure 3a). However, snow accumulation up to 10 cm may have significantly reduced light levels beneath the ice cover (Figure 3a).

The wavelet spectrum (Figures 3d, 3g, and 3j) shows a different origin of the subsurface (6–40 m) VBS maximum observed during the period of enhanced cell circulation. In contrast to the preceding and following periods, this maximum was mainly associated with a very weak intensity of the diurnal periodicity that was comparable in strength to that during polar night. The following period was characterized by rapid increase of the diurnal signal with wavelet spectrum energy rising from 50–70 to 200. This maximum was observed at all three moorings; however, the intensity of the diurnal signal decreased toward the YS mouth (Figures 3d, 3g, and 3j), which is in agreement with a general tendency of the VBS to be lower toward the YS entrance. From the last weeks of March to the beginning of polar day (17 April 2014), the diurnal periodicity gradually returned to a relatively weak mode with amplitudes comparable to those seen during polar night. Using wavelet analysis was problematic for separating 24.8 h lunar-day signal from diurnal one due to the close proximity of these periods.

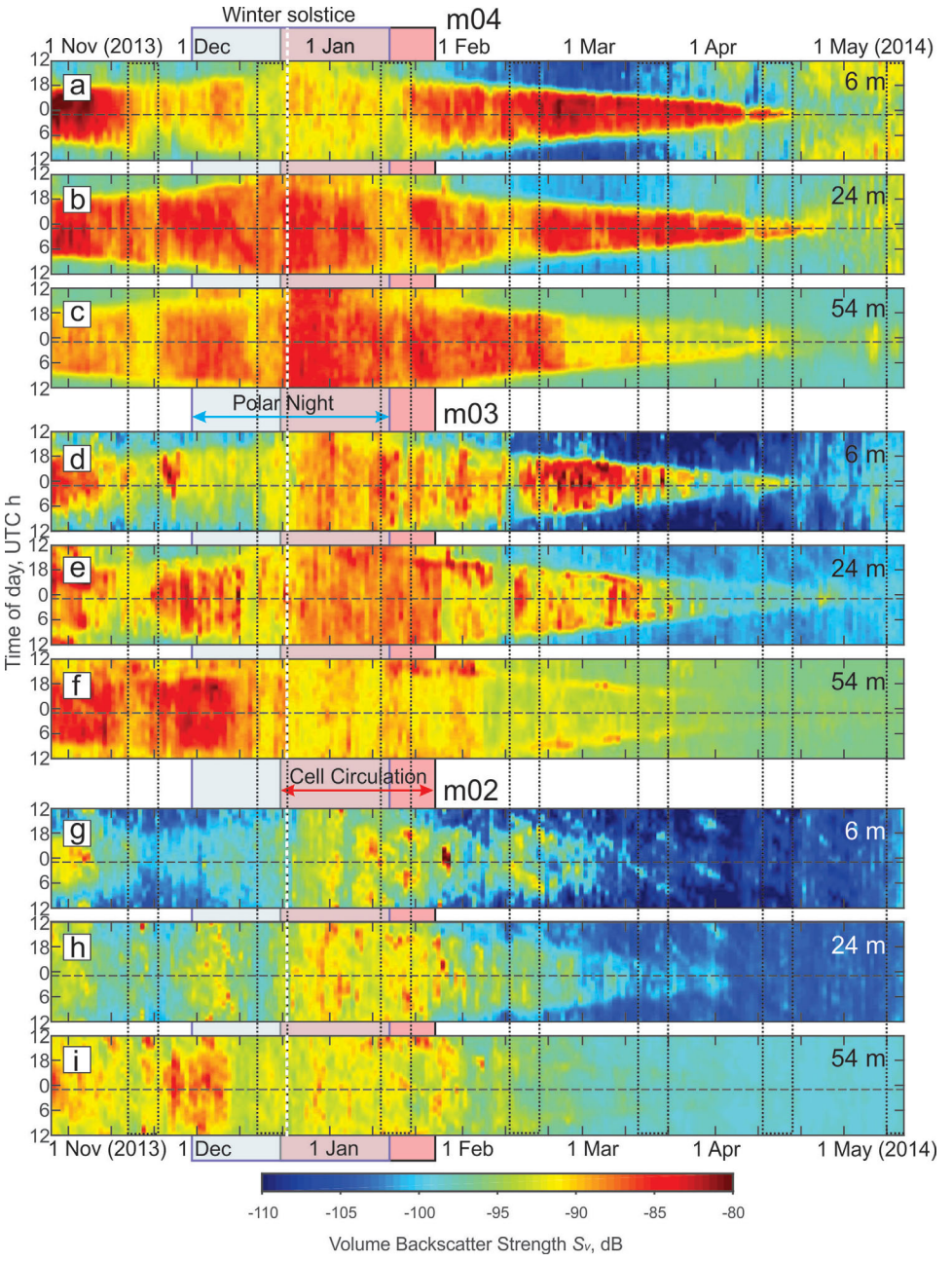

Figure 4. Actograms of the ADCP acoustic backscatter for (a, b, c) *m04*, (d, e, f) *m03*, and (g, h, j) *m02* moorings at three depth levels: (a, e, h) 6 m, (b, e, h) 24 m and (c, f, j) 54 m. Vertical white dashed line depicts winter solstice. Horizontal dashed line shows astronomic midnight. Dotted rectangular contours the full moon occurrence ±3 days. Color shading is similar to that in Figure 3.

VBS actograms were computed for the depth of 6, 24 and 54 m for all three moorings (Figure 4). These actograms reveal a rhythm of activity: where diurnal signal variations can be seen in the vertical axis of actogram, while the long-term patterns of diurnal behavior are revealed by variations along the horizontal axis [e. g., *Leise et al.*, 2013; *Last et al.*, 2016]. In general, these actograms display evidence for expanding the period of high VBS from the midnight in polar day to the entire 24-h period at winter solstice. They are nearly symmetric around the astronomic midnight (horizontal dashed line). However, during the period of enhanced cell circulation (20 December 2013 to 23 January 2015) induced by the polynya opening at the YS mouth, the diurnal periodicity of the signal was notably disrupted (Figure 4).

In contrast to the symmetry relative to the astronomic midnight, the actograms reveal asymmetry with respect to winter solstice (vertical white dashed line) that are consistent with wavelet results. At the *m2* and *m3* moorings, located closer to the mouth of the fjord, the diurnal cycle was indiscernible in the whole water column from about 10 days prior to about 30 days after winter solstice (Figure 4). This period showed a high VBS around −85 dB during the entire 24 h period. A weakening of the circulation cell was associated with the return of the diurnal signal from about 20 January 2014. Toward the polar day, the period of high VBS was gradually narrowing around the astronomic midnight until full disappearance on 18 April, which was simultaneously observed at *m04* and *m03* (Figures 4a–4f). At *m02*, the diurnal signal pattern was noticeably irregular and completely absent at 54 m depth (Figures 4g–4i).

3.2. Effect of the Moon

Another set of actograms was generated for modeled under ice illuminance (Figure 5a) and the ADCP-measured vertical velocity averaged for 16–30 m (above the interface) and 40–54 m (below the interface), respectively (Figures 5c–5h). The averaging over 14 m layers and over 7 ensembles (1 h) reduces velocity error estimates down to 2.2 mm/s, respectively. The bias correction for vertical velocity was performed according to *Plueddemann and Pinkel* [1989] and for each of three mooring was estimated around 0.2 mm/s. The vertical velocity actograms for *m04* and *m03* show a nearly symmetrical diurnal pattern around astronomic midnight (Figures 5c–5f) that is consistent with the backscatter actograms. Net upward flow was observed daily at *m04* from ∼1 to 8 h before the astronomic midnight during polar night. In the period between the polar night and day, upward flow was observed for 6–12 h per d during the period around midnight. In between, a net downward flow was observed (Figures 5c and 5d). A notable feature is that maximal velocities, exceeding ±0.3 cm/s, were recorded only during relatively brief ∼3 h periods prior to the change of direction of the vertical net flow. This feature is particularly noticeable in the period between polar night and day. This pattern completely disappeared after around 20 April 2014 when the polar day began. Mooring *m03* showed a similar pattern, but the signal was noisier and started to disappear already by the end of March. At *m02*, the mentioned patterns of vertical velocity were hardly recognizable.

Moonlight was the main source of continuous illumination during civil twilight and civil polar night in YS (Figure 5a) with maximum modeled values of illuminance around 9×10^{-2} lux. Even below the 35–85 cm sea ice with an up to 30 cm thick snow cover (Figure 3a), it was found the regular pattern of vertical velocity was disrupted during full moon, such that a weak but on average upward (positive) net flow was observed throughout the day (mooring *m04*, Figure 5c). Moreover, this disruption occurred only when the moon was above the horizon and illuminated the YS ice surface directly (compare Figure 5a and Figure 5c). This allows direct attribution of the diurnal cycle disruption to the moon illumination. The impact of the moon phase on the vertical velocity irregularities described above was obvious at *m04* (Figures 5c and 5d), recognizable at *m03* (Figures 5e and 5f) and fairly masked at *m02* (Figures 5g and 5h). At *m04*, the net upward flow in 16–30 m at the full moon (Figure 5c) was consistent with insignificant, but recognizable loss of VBS at 24 m (Figure 4b). However, it was not associated with gain in VBS at 6 m (Figure 4a). Thus, this allows for speculation that the backscattering zooplankton were redistributed to the surface layer that was not resolved by ADCP observations.

Additional evidence of the impact of the moon's illumination on disrupting the diurnal velocity signal arises from the cloud data. NCEP-derived cloud cover data have been found to be unreliable for high latitude regions [*Bedacht et al*., 2007], however, this data source is the only available information on clouds for the YS region. During the full moon on 14–20 December 2013, moon illumination was likely attenuated due to the ∼70% cloud cover (Figures 5a–5c). This resulted in a weaker disruption of the diurnal vertical velocity signal compared to the preceding quarter moon phase when the mean cloud cover was about 40%.

Our data revealed a noticeable difference in vertical velocity between the new and full moon phases during the fall transition to civil twilight. The time series of the 2 m binned vertical velocity profiles were computed for *m04* by averaging the individual velocity profiles recorded during the new moon phase, that occurred between 31 October and 6 November (Figure 6a), and full moon phase between 14 and 20 November 2013 (Figure 6b) with corresponding error margin of ∼0.5mm/s. Intensive downward and upward flow was observed during ∼3 h from 6 to 9 h and from 15 to 18 h, respectively. For the new moon, the vertical

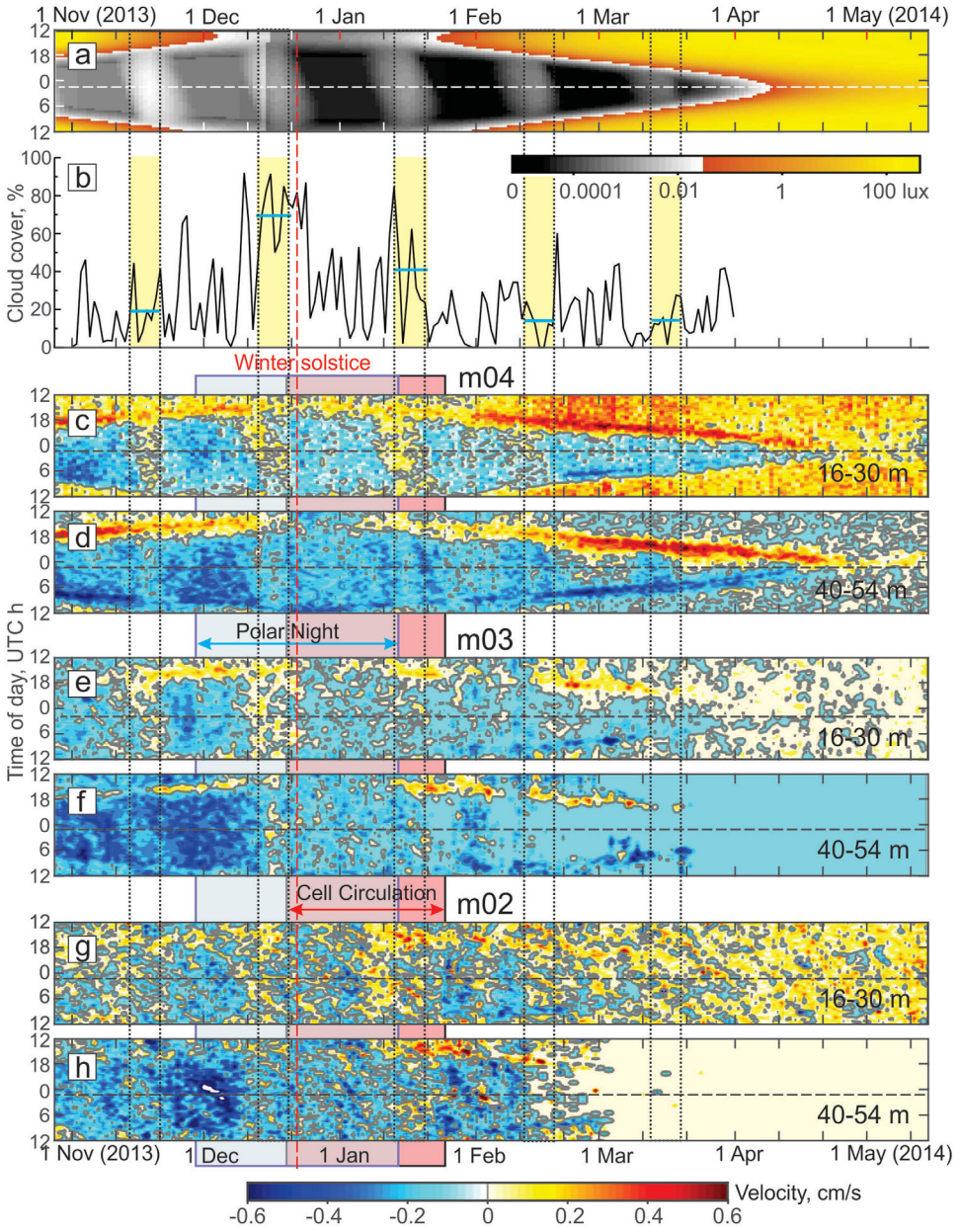

Figure 5. Actograms of the (a) modeled underice illuminance (lux) (c–h) ADCP-measured vertical velocity (cm/s) for (c, d) *m04*, (e, f) *m03*, and (g, h) *m02* moorings averaged for (c, e, g) 16–30 m and (d, f, h) 40–54m. Positive/negative values correspond to the upward/downward displacement. Color shading and designations are similar to that in Figures 3 and 4. (b) Time series of the NCEP-derived total cloud cover (%) with yellow shading highlighting the full moon occurrence ±4 days. The blue horizontal lines indicate the mean cloud cover for these periods. Dotted rectangular contours the full moon occurrence ±3 days.

velocities were about ±0.4–0.5 cm/s and the diurnal velocity signal was present already below 10 m depth. For the full moon, velocities were about half as much and the diurnal velocity signal was distinguishable only at depth below 25 m which is consistent with Figures 5a and 5b.

The vertical velocities seen in Figure 6 are consistent with active backscatters moving up- and down through the water column with diurnal periodicity. From the velocity distribution in Figure 6a, an approximation has been made for the vertical upward and downward movement following the maximal velocities (white solid lines in Figure 6a). This approximation allowed estimations of the vertical displacement velocities of ∼1.5 cm/s.

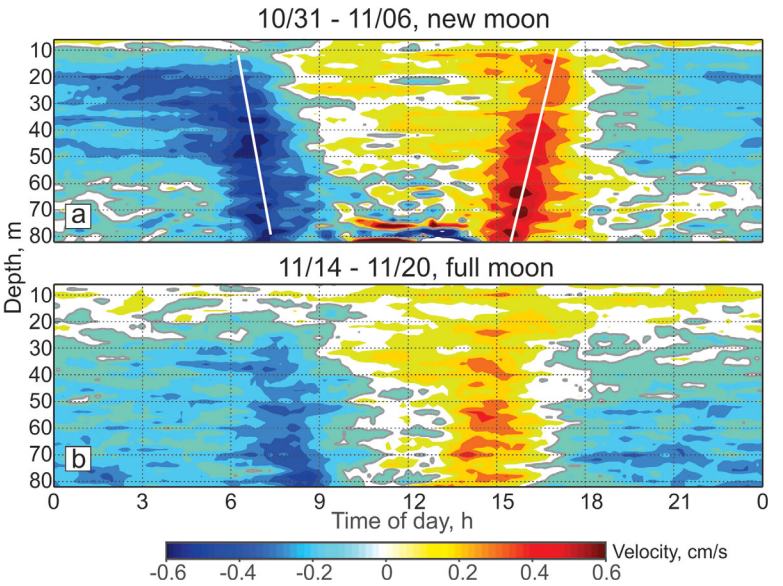

Figure 6. The time series of 2 m binned vertical profiles of vertical velocity (cm/s) averaged over the (a) new moon phase (31 October to 6 November2013) and (b) full moon phase (14–20 November 2013) for mooring *m04*. Positive/negative values correspond to the upward/downward displacement. White line approximates vertical movement attributed to DVM.

4. Discussion

4.1. Possible Species Associated With DVM

The observed patterns of the ADCP-derived VBS and vertical velocity below the land-fast ice during winter 2013–2014 were consistent with diel vertical migration (DVM) of zooplankton, during which zooplankton moved toward the surface during the evening, and descends the next morning. Without zooplankton sampling, it was not possible for us to specify the exact species involved in DVM [*Cottier et al*., 2006; *Falk-Petersen and Hopkins*, 1981; *Falk-Petersen and Kristensen*, 1985; *Falk-Petersen et al*., 2008; *Vestheim et al*., 2014], and hence we follow those studies that use only acoustical methods to determine and interpret the patterns of the DVM signal [e.g., *Fischer and Visbeck*, 1993; *Berge et al*., 2009].

Precise identification of zooplankton species is not possible just from acoustic data. However, based on previous studies the possible species involved in DVM could be surmised with some confidence. ADCP velocity observations detect the presence of relatively fast moving animals with vertical velocities of ~1.5 cm/s that migrate to ~80 m or deeper (Figure 6). Krill (*Euphausiacea*) and *Themisto* are known to move down to 100–300 m depth in DVM at 70°N [*Falk-Petersen and Hopkins*, 1981; *Vestheim et al*., 2014]. The estimated vertical migration speed fits nicely into the range of 1–6 cm/s characteristic for copepods and euphausiids [*Heywood*, 1996]. Previous zooplankton sampling in YS [*Rysgaard et al*., 1999; *Nielsen et al*., 2007; *Arendt et al*., 2013] revealed an abundant community of copepods. These studies found that among the copepods, *Microstella norvegica* constituted 32–49% or 5000–10,000 ind/m^3, while *Calanus* spp. constituted 9–24%. Among the non-copepods, krill comprised about 70 ind/m^3 and *Themisto* just 0.1 ind/m^3. Krill is expected to be very abundant in east Greenland fjords, and *Thysanoessa inermis* and *Meganytiphanes norvegica* was also recorded in high number by *Einarsson* [1945] during the warm 1930s. Small copepods as *Oithona, Microcalanus, Microstella* are too small (less than 1.5 mm) to be recorded by ADCP and does not perform large seasonal migration [*Darnis and Fortier*, 2014] or measurable DVM (G. Darnis, personal communication, 2014) in Arctic waters. *Calanus* species perform seasonal vertical migration and the larger part of the population stays at depth, below those investigated in this study, from early autumn to late spring [*Falk-Petersen et al*., 2007]. *Berge et al*. [2014] also concluded, based on comparison between acoustic and net data, that the acoustic backscatter signal from *Calanus* copepods is typically overwhelmed by the signal from larger zooplankton species such as krill and pelagic amphipods. We therefore suggest that krill and possibly *Themisto* were the main scatters in the backscatter signal.

4.2. Disruption of Under-Ice DVM by Polynya Formation

The DVM signal was observed to be disrupted during polynya-enhanced cell circulation. The VBS signal at the moorings *m02* and *m03* located closer to the mouth of the fjord, indicated that the bulk of the zooplankton continuously occupied the subsurface layer (Figures 3f and 3i). The significant disruption of the DVM signal during the polynya-enhanced cell circulation was also evident for 6 m and 24 m depths at m04 (Figures 4d and 4e) and *m02* (Figures 4g and 4h). The difference in DVM-signal between moorings in the mouth of the fjord (*m02* and *m03*) and the one in the fjord's interior (*m04*) could possibly be attributed to differences in zooplankton species composition or their age composition. Even though fjords are semienclosed water bodies, they can be very dynamic and variable. In their study at 70°N *Falk-Petersen and Kristensen* [1985] showed that the biomass, distribution and behavior of the dominant krill species changed with topography and distance from the entrance and head of the fjord. This was probably related to the fjord circulation and hydrographic regimes.

The period of DVM disruption matches the cell-circulation period. In the following, we propose two possible explanations for the irregular behavior of zooplankton associated with enhanced water dynamics.

1. During the polynya event over the YS mouth, the along fjord inflow/outflow maximum velocities temporally exceeded 7/12 cm/s (Figures 3b, 3e, and 3h) thereby creating an enhanced velocity gradient across the interface at ~40 m (depth of sill) between the inflow in the intermediate layer at ~40–140 m and outflow in the subsurface layer at ~6–40 m (Figure 1a). Based on the observed patterns, it therefore appears that the zooplankton avoided spending additional energy crossing this interface for regular DVM and preferred to remain in the subsurface layer. Besides predator and starvation avoidance, this strategy of minimizing energy use due to advection in the case of enhanced water dynamics was previously reported by *Eiane et al*. [1998], *Basedow et al*. [2004], and *Marcus and Scheef* [2009].
2. The polynya-enhanced cell circulation was accompanied by a relative increase in temperature of the subsurface layer (from an average of −1.76°C up to −1.70 f°C) that resulted in the upward heat flux to the ice-water interface by up to 22–24 W/m^2 at the outer fjord (moorings *m02* and *m03*) and up to 14.5 W/m^2 in the inner fjord (mooring *m04*) [*Kirillov et al*., 2015]. The relatively strong thermal gradient, observed by *Dmitrenko et al*. [2015] between the warmer upper layer above the 40 m depth and deeper waters may have caused zooplankton to favor the upper water layer.

4.3. Disruption of Under-Ice DVM by the Moon Cycle

In addition to water dynamics, another disrupting factor for DVM was the moon cycle. Most studies on lunar disruption of DVM were conducted either at subtropical latitudes [*Hernández-León et al*., 2002] or in the deep sea [*Mercier et al*., 2011; *Ochoa et al*., 2013]. In general, DVM patterns are known to correlate well with the moon phase [*Ochoa et al*., 2013; *van Haren and Compton*, 2013]. Herbivorous zooplankton species are typically observed maintaining deeper positions in the water column during the full moon phase, whereas they are more abundant in the surface water layer during new moon phase. This behavior helps avoiding predation and offers reproductive benefits [*Marcus and Scheef*, 2009]. In contrast to lower latitudes, very little is known about the exact mechanism of how the moon cycle exert control over DVM during polar night [*Berge et al*., 2015a; *Webster et al*., 2015]. A recent study conducted by *Last et al*. [2016] over the open water nearby Svalbard showed DVM disruption by lunar cycle during polar night. They reported that variation in the zooplankton layer depth within the surface layer (~50 m) correlated with lunar altitude periodicity (24.8 hrs) and that zooplankton practice surface avoidance. *Last et al*. [2016] also reported evidence of two distinct lunar vertical migration (LVM) patterns: LVM-month and LVM-day, both occurring in ice covered waters. Our VBS actograms did not show distinguishable asymmetry around midnight and the slanted pattern described by *Last et al*. [2016] as-day that corresponds with the shifting of periodicity from 24 hr to 24.8 hr.

Our under-ice VBS data revealed that the DVM signal pattern also was disrupted during full moon phases (Figure 5). The zooplankton, that were the likely cause of the VBS signal, appeared to be more distributed within the upper layer below the sea-ice during full moon. This signal was relatively weak, but remained detectable at *m03* and *m04* during the snow free period (Figures 3a–3e). During the full moon, the vertical velocity observations indicated near-zero (~0.01 cm/s) diel-independent net velocities (Figures 5c–5e), which supports the lack of coordinated movement by zooplankton. Specifically, no DVM was observed to occur in the subsurface layer down to 20–30 m depth during the full moon stage (Figure 6b). However,

below 30 m depth the vertical velocity profiles gave evidence for a weaker, but still well recognizable DVM, which may have been related to a transition in light levels below a threshold of predator's perception at that depth.

The possible reasons for the lunar disruption of DVM are uncertain. The upward migration of zooplankton at full moon could be associated with exploitation strategies of food resources. It is known that krill can feed on decaying phytoplankton both on the under ice surface and bottom sediment [*Falk-Petersen et al*., 2000]. During polar night below 65–85 cm thick land-fast ice, lunar illumination is likely to be far below the threshold of the predators' perception. This significantly reduces the light-dependent mortality risk and gives zooplankton favorable conditions for predator avoidance. At the same time, the faint lunar illumination could be used by the otherwise migrating zooplankton for optimizing their exploitation of food resources during polar night when access to illumination is extremely limited.

The VBS and its wavelet transform analysis provided definite evidence that zooplankton were performing DVM outside the full moon and enhanced cell circulation periods (Figure 3). This imposes an open question: What drives DVM in polar night during the new moon phase when illumination in the ocean is below the perception threshold for many living creatures or practically absent. One possible explanation is the presence of an internal clock mechanism [e.g., *van Haren and Compton*, 2013, *Cisewski and Strass*, 2016] that keeps up the DVM cycle even when there is no illumination. The VBS actograms (Figure 4) show noticeable symmetry of DVM signal relative to astronomic midnight during polar night, the period when the sun is 6° below horizon at its highest point. In Young Sound there is additional shading by the mountains. This symmetry might therefore be interpreted into favor of an internal clock mechanism.

Another explanation is the theory that the plankton possess an outstanding sensitivity to the light levels far below the threshold of human perception [*Berge et al*., 2014; *Cohen et al*., 2015]. During the full moon phases our modeled illuminance under the sea ice cover in Young Sound indicated that values could reached 2×10^{-3} lux. *Båtnes et al*. [2015] reported that *Calanus* had sensitivity to illuminance levels as low as 5×10^{-8} μmol photons m^{-2} s^{-1} for blue waveband which corresponds with about 3×10^{-6} lux. Similar light sensitivity for *Krill* were reported by *Cohen et al*. [2015].

5. Conclusions

Time series of acoustic backscatter and velocity from three ADCPs deployed from late October 2013 to May 2014 in the Young Sound fjord in Northeast Greenland were used to analyze patterns of diel vertical migration (DVM) in the water column beneath land-fast sea ice cover.

Our analysis was limited by the lack of the zooplankton sampling. The deficiency of this analysis clearly defines a necessity for expanding the investigation of zooplankton DVM dynamics in high latitudes ice-covered waters using observations of cloud coverage, incident and subice light climate, zooplankton species composition in addition to ADCP and ABS observations. We also limited our analysis be neglecting the export of zooplankton away from YS during the enhanced estuarine-like circulation in December 2013 to January 2014.

In contrast to many previous studies of the high Arctic regions, the DVM signal in Young Sound persisted throughout the entire winter and even during the period of polar night. However, the DVM signal was significantly disrupted (i) by estuarine-like water dynamics enhanced by a polynya forming over the Young Sound outlet to the Greenland Sea and (ii) during the full moon phase of the moon cycle.

1. *Disruption by water dynamics*: Our data suggest that the zooplankton species likely responsible for DVM tended to avoid spending additional energy crossing the interface at around 40 m depth between inflow to the fjord in the intermediate layer and outflow in the subsurface layer where a relatively strong velocity gradient was observed. Instead the zooplankton tended to favor remaining in the upper 40 m where also the relatively warmer water temperatures.
2. *Disruption by moon light*: During civil twilight and civil polar night, moonlight is the major significant source of illumination besides stars and aurora borealis. During full moon phases, the VBS and vertical velocity observations revealed that the 1999 signal was disrupted and zooplankton were homogeneously redistributed within the upper layer below the 60–90 cm thick land-fast sea ice with ~10 cm snow cover. This signal tends to disappear at high cloud and snow cover. Our modeled analysis suggests that

the zooplankton in question have an outstanding sensitivity to illuminance levels of 0.002 lux and less. We speculate that this extraordinary sensitivity favors zooplankton to harvest and avoid predation below the land-fast ice during polar night during full moon phases thereby reducing their light-dependent mortality risk.

Acknowledgments
This study was funded by the Canada Excellence Research Chair (CERC) program, the Canada Research Chair (CRC) program, the Canada Foundation of Innovation (CFI), the National Sciences and Engineering Research Council of Canada (NSERC, grant RGPIN-2014-03606), the Manitoba Research and Innovation Fund, and the University of Manitoba, Aarhus University and the Greenland Institute of Natural Resources. We thank Ivali Lennert, Kunuk Lennert and Egon Frandsen for outstanding technical assistance in the field. We also thank Jørgen Berge and another anonymous reviewer for their constructive comments. This work is a contribution to the Arctic Science Partnership (ASP) and the ArcticNet Networks of Centres of Excellence programs. Stig Falk-Petersen was funded by the Research Council of Norway through the projects Marine Night (226417). The meteorological, CTD, and velocity data archived in the Centre for Earth Observation Science (University of Manitoba) is restricted for open access during 2 years after the observations completed. Afterward it will be posted on the ASP webpage at http://www.asp-net.org.

References

Arendt, K. E., T. Juul-Pedersen, J. Mortensen, M. E. Blicher, and S. Rysgaard (2013), A 5-year study of seasonal patterns in mesozooplankton community structure in a sub-Arctic fjord reveals dominance of Microsetella norvegica (Crustacea, Copepoda), *J. Plankton Res.*, *35*, 105–120, doi:10.1093/plankt/fbs087.

Babb, D. G., R. J. Galley, D. G. Barber, and S. Rysgaard (2016), Physical processes contributing to an ice free Beaufort Sea during September 2012, *J. Geophys. Res. Oceans*, *120*, 267–283, doi:10.1002/2015JC010756.

Basedow, S., K. Eiane, V. Tverberg, and M. Spindler (2004), Advection of zooplankton in an Arctic fjord (Kongsfjorden, Svalbard), *Estuarine Coastal Shelf Sci.*, *60*(1), 113–124, doi:10.1016/j.ecss.2003.12.004.

Båtnes, A. S., C. Miljeteig, J. Berge, M. Greenacre, and G. Johnsen (2015), Quantifying the light sensitivity of Calanus spp. during the polar night: Potential for orchestrated migrations conducted by ambient light from the sun, moon, or aurora borealis?, *Polar Biol.*, *38*(1), 51–65, doi:10.1007/s00300-013-1415-4.

Bedacht, E., S. K. Gulev, and A. Macke (2007), Intercomparison of global cloud cover fields over oceans from the VOS observations and NCEP/NCAR reanalysis, *Int. J. Climatol.*, *27*(13), 1707–1719, doi:10.1002/joc.1490.

Bendtsen, J., K. E. Gustafsson, S. Rysgaard, and T. Vang (2007), Physical conditions, dynamics and model simulations during the ice-free period of the Young Sound/Tyrolerfjord system, in *Carbon Cycling in Arctic Marine Ecosystems: Case Study Young Sound*, vol. 58, edited by S. Rysgaard and R. N. Glud, pp. 46–59, Meddelelser om Grønland, Nuuk, Greenland.

Benoit, D., Y. Simard, J. Gagné, M. Geoffroy, and L. Fortier (2010), From polar night to midnight sun: Photoperiod, seal predation, and the diel vertical migrations of polar cod (Boreogadus saida) under landfast ice in the Arctic Ocean, *Polar Biol.*, *33*(11), 1505–1520, doi:10.1007/s00300-010-0840-x.

Berge, J., et al. (2009), Diel vertical migration of Arctic zooplankton during the polar night, *Biol. Lett.*, *5*(1), 69–72, doi:10.1098/rsbl.2008.0484.

Berge, J., A. S. Båtnes, G. Johnsen, S. M. Blackwell, and M. A. Moline (2012), Bioluminescence in the high Arctic during the polar night., *Mar. Biol.*, *159*(1), 231–237, doi:10.1007/s00227-011-1798-0.

Berge, J., et al. (2014), Arctic complexity: A case study on diel vertical migration of zooplankton., *J. Plankton Res.*, *36*(5), 1279–1297, doi:10.1093/plankt/fbu059.

Berge, J., et al. (2015a), In the dark: A review of ecosystem processes during the Arctic polar night, *Prog. Oceanogr.*, *139*, 258–271, doi:10.1016/j.pocean.2015.08.005.

Berge, J., et al. (2015b), Unexpected levels of biological activity during the Polar night offer new perspectives on a warming Arctic, *Curr. Biol.*, *25*(19), 2555–2561, doi:10.1016/j.cub.2015.08.024.

Blachowiak-Samolyk, K., S. Kwasniewski, K. Richardson, K. Dmoch, E. Hansen, H. Hop, S. Falk-Petersen, and L. T. Mouritsen (2006), Arctic zooplankton do not perform diel vertical migration (DVM) during periods of midnight sun, *Mar. Ecol. Prog. Ser.*, *308*, 101–116, doi:10.3354/meps308101.

Bozzano, R., E. Fanelli, S. Pensieri, P. Picco, and M. E. Schiano (2014), Temporal variations of zooplankton biomass in the Ligurian Sea inferred from long time series of ADCP data, *Ocean Sci.*, *10*(1), 93–105, doi:10.5194/os-10-93-2014.

Brierley, A. S. (2014), Diel vertical migration, *Curr. Biol.*, *24*(22), R1074–R1076, doi:10.1016/j.cub.2014.08.054.

Brierley, A. S., M. A. Brandon, and J. L. Watkins (1998), An assessment of the utility of an acoustic Doppler current profiler for biomass estimation, *Deep Sea Res., Part I*, *45*(9), 1555–1573, doi:10.1016/S0967-0637(98)00012-0.

Brierley, A. S., R. A. Saunders, D. G. Bone, E. J. Murphy, P. Enderlein, S. G. Conti, and D. A. Demer (2006), Use of moored acoustic instruments to measure short-term variability in abundance of Antarctic krill, *Limnol. Oceanogr. Methods*, *4*(2), 18–29, doi:10.4319/lom.2006.4.18.

Chenghao, Y., L. Guanghong, Y. Yaochu, C. Hong, and Z. H. U. Xiaohua (2013), The diel vertical migration of sound scatterers observed by an acoustic Doppler current profiler in the Luzon Strait from July 2009 to April 2011, *Acta Oceanol. Sin.*, *32*(11), 1–9.

Cisewski, B., and V. H. Strass (2016), Acoustic insights into the zooplankton dynamics of the eastern Weddell Sea, *Prog. Oceanogr.*, *144*, 62–92, doi:10.1016/j.pocean.2016.03.005.

Cohen, J. H., et al. (2015), Is ambient light during the high arctic Polar Night sufficient to act as a visual cue for zooplankton?, *PLoS One*, *10*(6), e0126247, doi:10.1371/journal.pone.0126247.

Cottier, F. R., G. A. Tarling, A. Wold, and S. Falk-Petersen (2006), Unsynchronized and synchronized vertical migration of zooplankton in a high arctic fjord, *Limnol. Oceanogr. Methods*, *51*(6), 2586–2599, doi:10.4319/lo.2006.51.6.2586.

Cottier, F. R., F. Nilsen, R. Skogseth, V. Tverberg, J. Skarthhamar, and H. Svendsen (2010), Arctic fjords: A review of the oceanographic environment and dominant physical processes, *Geol. Soc. Spec. Publ.*, *344*, 35–50, doi:10.1144/SP344.4.

Darnis, G., and L. Fortier (2014), Temperature, food and the seasonal vertical migration of key arctic copepods in the thermally stratified Amundsen Gulf (Beaufort Sea, Arctic Ocean), *J. Plankton Res.*, *36*(4), 1092–1108, doi:10.1093/plankt/fbu035.

Deines, K. L. (1999), Backscatter estimation using Broadband acoustic Doppler current profilers, in *Proceedings of the IEEE Sixth Working Conference on Current Measurement (Cat. No.99CH36331)*, pp. 249–253, IEEE, San Diego, Calif.

Dmitrenko, I. A., S. A. Kirillov, S. Rysgaard, D. G. Barber, D. G. Babb, L. T. Pedersen, N. V. Koldunov, W. Boone, O. Crabeck, and J. Mortensen (2015), Polynya impacts on water properties in a Northeast Greenland Fiord, *Estuarine Coastal Shelf Sci.*, 153, 10–17, doi:10.1016/j.ecss.2014.11.027.

Doney, S. C., and D. K. Steinberg (2013), Marine biogeochemistry: The ups and downs of ocean oxygen, *Nat. Geosci.*, *6*(7), 515–516, doi:10.1038/ngeo1872.

Eiane, K., D. Aksnes, and M. Ohman (1998), Advection and zooplankton fitness, *SARSIA*, *83*, 87–93, doi:10.1080/00364827.1998.10413674.

Einarsson, H. (1945), Northern Atlantic Species, in *Euphausiacea*, vol. 27, edited by B. Luno, 191 pp., Copenhagen.

Falk-Petersen, S., and C. C. E. Hopkins (1981), Zoo plankton sound scattering layers in North Norwegian Fjords interactions between fish and krill shoals in a winter situation in Ullsfjorden And Oksfjorden Norway, in *15th European Marine Biology Symposium: Lower Organisms And Their Role In The Food Web*, edited by G. Rheinheimer, et al., pp. 191–201, Institut für Meereskunde an der Universität Kiel, Kiel.

Falk-Petersen, S., and A. Kristensen (1985), Acoustic assessment of krill stocks in Ullsfjorden, North Norway, *SARSIA*, *70*(1), 83–90.

Falk-Petersen, S., W. Hagen, G. Kattner, A. Clarke, and J. Sargent (2000), Lipids, trophic relationships, and biodiversity in Arctic and Antarctic krill, *Can. J. Fish. Aquat. Sci.*, *57*, 178–191, doi:10.1139/f00-194.

Falk-Petersen, S., V. Pavlov, S. Timofeev, and J. Sargent (2007), Climate variability and possible effects on arctic food chains: The role of Calanus, in *Arctic Alpine Ecosystems and People in a Changing Environment*, edited by J. Ørbæk et al., pp. 147–166, Springer, Berlin.

Falk-Petersen, S., et al. (2008), Vertical migration in high Arctic waters during autumn 2004, *Deep Sea Res., Part II*, *55*(20-21), 2275–2284, doi:10.1016/j.dsr2.2008.05.010.

Farmer, D. M., and H. J. Freeland (1983), The physical oceanography of fjords, *Prog. Oceanogr.*, *12*, 147–220.

Fielding, S., G. Griffiths, and H. S. J. Roe (2004), The biological validation of ADCP acoustic backscatter through direct comparison with net samples and model predictions based on acoustic-scattering models, *ICES J. Mar. Sci.*, *61*(2), 184–200, doi:10.1016/j.icesjms.2003.10.011.

Fischer, J., and M. Visbeck (1993), Seasonal variation of the daily zooplankton migration in the Greenland sea, *Deep Sea Res., Part I*, *40*, 1547–1557, doi:10.1016/0967-0637(93)90015-U.

Flagg, C. N., and S. L. Smith (1989), On the use of the acoustic Doppler current profiler to measure zooplankton abundance, *Deep Sea Res., Part A*, *36*(3), 455–474, doi:10.1016/0198-0149(89)90047-2.

Foreman, M. G. G. (1978), *Manual For Tidal Currents Analysis And Prediction*, Pacific Marine Science Report 78-6, Institute of Ocean Sciences, Sidney, BC.

Fortier, M. (2001), Visual predators and the diel vertical migration of copepods under Arctic sea ice during the midnight sun, *J. Plankton Res.*, *23*(11), 1263–1278, doi:10.1093/plankt/23.11.1263.

Grenfell, C. G., and G. A. Maykut (1977), The optical properties of ice and snow in the Arctic Basin, *J. Glaciol.*, *18*(80), 445–463.

Hamilton, J. M., K. Collins, and S. J. Prinsenberg (2013), Links between ocean properties, ice cover, and plankton dynamics on interannual time scales in the Canadian Arctic Archipelago, *J. Geophys. Res. Oceans*, *118*, 5625–5639, doi:10.1002/jgrc.20382.

Hays, G. C. (2003), A review of the adaptive significance and ecosystem consequences of zooplankton diel vertical migrations, *Hydrobiologia*, *503*(1-3), 163–170, doi:10.1023/B:HYDR.0000008476.23617.b0.

Hernández-León, S., C. Almeida, L. Yebra, and J. Arístegui (2002), Lunar cycle of zooplankton biomass in subtropical waters: Biogeochemical implications, *J. Plankton Res.*, *24*(9), 935–939, doi:10.1093/plankt/24.9.935.

Heywood, K. J. (1996), Diel vertical migration of zooplankton in the Northeast Atlantic, *J. Plankton Res.*, *18*(2), 163–184, doi:10.1093/plankt/18.2.163.

Jasek, M., and J. Marko (2007), Instrument for detecting suspended and surface ice runs in rivers, paper presented at *14th Workshop on the Hydraulics of Ice Covered Rivers*, CGU HS Committee on River Ice Processes and the Environment, Quebec City, Canada.

Kerfoot, W. C. (1985), Adaptive value of vertical migration: Comments on the predation hypothesis and some alternatives., in *Contributions in Marine Science*, vol. 27, edited by M. A. Rankin, pp. 91–113, Univ. of Tex., Port Aransas.

Kirillov, S., I. Dmitrenko, D. Babb, S. Rysgaard, and D. Barber (2015), The effect of ocean heat flux on seasonal ice growth in Young Sound (Northeast Greenland), *J. Geophys. Res. Oceans*, *120*, 4803–4824, doi:10.1002/2015JC010720.

Kosobokova, K. N. (1978), Diurnal vertical distribution of Calanus Hyperboreus Kroyer and Calanus Glacialis Jaschnov in Central Polar Basin, *Okeanologiya*, *18*(4), 722–728.

Kumar, P., and E. Foufoula-Georgiou (1997), Wavelet analysis for geophysical applications, *Rev. Geophys.*, *35*(4), 385–412, doi:10.1029/97RG00427.

Lampert, W. (1989), The adaptive significance of diel vertical migration of zooplankton, *Funct. Ecol.*, *3*, 21–27.

Last, K. S., L. Hobbs, J. Berge, A. S. Brierley, and F. Cottier (2016), Moonlight drives ocean-scale mass vertical migration of zooplankton during the Arctic Winter, *Curr. Biol.*, *26*(2), 244–251, doi:10.1016/j.cub.2015.11.038.

Leise, T. L., P. Indic, M. J. Paul, and W. J. Schwartz (2013), Wavelet meets actogram, *J. Biol. Rhythms*, *28*(1), 62–68, doi:10.1177/0748730412468693.

Lemon, D. D., D. Billenness, and J. Buermans (2008), Comparison of acoustic measurements of zooplankton populations using an Acoustic Water Column Profiler and an ADCP, in *OCEANS 2008*, pp. 1–8, IEEE Oceanic Engineering Society, Quebec City, QC.

MacCready, P., and W. R. Geyer (2009), Advances in estuarine physics, *Annu. Rev. Mar. Sci.*, *2*(1), 35–58, doi:10.1146/annurev-marine-120308-081015.

Marcus, N. H., and L. P. Scheef (2009), Photoperiodism in Copepods, in *Photoperiodism: The Biological Calendar*, edited by R. J. Nelson, D. L. Denlinger, and D. E. Sommers, pp. 193–217, Oxford University Press, Oxford, U. K.

Mercier, A., Z. Sun, S. Baillon, and J.-F. Hamel (2011), Lunar rhythms in the deep sea: Evidence from the reproductive periodicity of several marine invertebrates., *J. Biol. Rhythms*, *26*(1), 82–86, doi:10.1177/0748730410391948.

Miller, G. S. (2003), Mysis Vertical Migration in Grand Traverse Bay, Lake Michigan, Observed by an Acoustic Doppler Current Profiler, *J. Great Lakes Res.*, *29*(3), 427–435, doi:10.1016/S0380-1330(03)70448-1.

Morlet, J., G. Arens, E. Fourgeau, and D. Giard (1982a), Wave propagation and sampling theory; Part II, Sampling theory and complex waves, *Geophysics*, *47*(2), 222–236, doi:10.1190/1.1441329.

Morlet, J., G. Arens, E. Fourgeau, and D. Giard (1982b), Wave propagation and sampling theory—Part I: Complex signal and scattering in multilayered media, *Geophysics*, *47*(2), 203, doi:10.1190/1.1441328.

Nielsen, T. G., L. D. Ottosen, and B. W. Hansen (2007), Structure and function of the pelagic ecosystem in Young Sound, NE Greenland, in *Carbon cycling in Arctic Marine Ecosystems: Case Study Young Sound*, vol. 58, edited by R. N. G. Søren Rysgaard, pp. 58–107, Meddelelser om Groenland. Bioscience, Nuuk, Greenland.

Ochoa, J., H. Maske, J. Sheinbaum, and J. Candela (2013), Diel and lunar cycles of vertical migration extending to below 1000 m in the ocean and the vertical connectivity of depth-tiered populations, *Limnol. Oceanogr. Methods*, *58*(4), 1207–1214, doi:10.4319/lo.2013.58.4.1207.

Ofek, E. O. (2014), MATLAB package for astronomy and astrophysics, *Astrophys. Source Code Libr. Rec. ascl1407.005*, doi:2014ascl.soft07005O.

Perovich, D. K. (1996), The optical properties of sea ice, *CRREL Monogr.*, *96-1*, 25.

Pinot, J. M., and J. Jansá (2001), Time variability of acoustic backscatter from zooplankton in the Ibiza Channel (western Mediterranean), *Deep. Sea Res., Part I*, *48*, 1651–1670, doi:10.1016/S0967-0637(00)00095-9.

Plueddemann, A. J., and R. Pinkel (1989), Characterization of the patterns of diel migration using a Doppler sonar, *Deep Sea Res., Part A*, *36*, 509–530, doi:10.1016/0198-0149(89)90003-4.

Rabindranath, A., M. Daase, S. Falk-Petersen, A. Wold, M. I. Wallace, J. Berge, and A. S. Brierley (2010), Seasonal and diel vertical migration of zooplankton in the High Arctic during the autumn midnight sun of 2008, *Mar. Biodiversity*, *41*(3), 365–382, doi:10.1007/s12526-010-0067-7.

Ringelberg, J. (2010), *Diel Vertical Migration of Zooplankton in Lakes and Oceans*, Springer Netherlands, Dordrecht.

Rysgaard, S., T. G. Nielsen, and B. W. Hansen (1999), Seasonal variation in nutrients, pelagic primary production and grazing in a high-Arctic coastal marine ecosystem, Young Sound, Northeast Greenland, *Mar. Ecol. Prog. Ser.*, *179*, 13–25, doi:10.3354/meps179013.

Sato, M., J. F. Dower, E. Kunze, and R. Dewey (2013), Second-order seasonal variability in diel vertical migration timing of euphausiids in a coastal inlet, *Mar. Ecol. Prog. Ser.*, *480*, 39–56, doi:10.3354/meps10215.

Skarðhamar, J., and H. Svendsen (2010), Short-term hydrographic variability in a stratified Arctic fjord, *Geol. Soc. Spec. Publ.*, *344*, 51–60, doi:10.1144/SP344.5.

Stanton, T. K., P. H. Wiebe, D. Chu, M. C. Benfield, L. Scanlon, L. Martin, and R. L. Eastwood (1994), On acoustic estimates of zooplankton biomass, *ICES J. Mar. Sci.*, *51*(4), 505–512, doi:10.1006/jmsc.1994.1051.

Stigebrandt, A. (2012), Hydrodynamics and circulation of fjords, in *Encyclopedia of Lakes and Reservoirs*, edited by L. Bengtsson, R. W. Herschy, and R. W. Fairbridge, pp. 327–344, Springer, Dordrecht, Netherlands.

Sutherland, D. A., F. Straneo, and R. S. Pickart (2014), Characteristics and dynamics of two major Greenland glacial fjords, *J. Geophys. Res. Oceans*, *119*, 3767–3791, doi:10.1002/2013JC009786.

Torgersen, T. (2003), Proximate causes for anti-predatory feeding suppression by zooplankton during the day: Reduction of contrast or motion–ingestion or clearance?, *J. Plankton Res.*, *25*(5), 565–571, doi:10.1093/plankt/25.5.565.

van Haren, H., and T. J. Compton (2013), Diel vertical migration in deep sea plankton is finely tuned to latitudinal and seasonal day length., edited by A. Davies, *PLoS One*, *8*(5), e64435, doi:10.1371/journal.pone.0064435.

Vestheim, H., A. Røstad, T. A. Klevjer, I. Solberg, and S. Kaartvedt (2014), Vertical distribution and diel vertical migration of krill beneath snow-covered ice and in ice-free waters, *J. Plankton Res.*, *36*(2), 503–512, doi:10.1093/plankt/fbt112.

Wallace, M. I., F. R. Cottier, J. Berge, G. a. Tarling, C. Griffiths, and A. S. Brierley (2010), Comparison of zooplankton vertical migration in an ice-free and a seasonally ice-covered Arctic fjord: An insight into the influence of sea ice cover on zooplankton behaviour, *Limnol. Oceanogr. Methods*, *55*(2), 831–845, doi:10.4319/lo.2009.55.2.0831.

Webster, C., Ø. Varpe, S. Falk-Petersen, J. Berge, E. Stübner, and A. Brierley (2015), Moonlit swimming: Vertical distributions of macrozooplankton and nekton during the polar night, *Polar Biol.*, *38*(1), 75–85, doi:10.1007/s00300-013-1422-5.

Zaret, T. M., and S. Suffern (1976), Vertical migration in zooplankton as a predator avoidance mechanism, *Limnol. Oceanogr.*, *21*(6), 804–813, doi:10.4319/lo.1976.21.6.0804.